

Effect of Rehybridization on the Electronic Structure of Single-Walled Carbon Nanotubes

M. A. Hamon,[†] M. E. Itkis,[†] S. Niyogi,[†] T. Alvaraez,[‡]
C. Kuper,[‡] M. Menon,[§] and R. C. Haddon^{*,†}

Departments of Chemistry and
Chemical and Environmental Engineering
University of California, Riverside, California 92521-0403
Versilant Nanotechnologies LLC
1520 Spruce Street Suite 703
Philadelphia, Pennsylvania 19102
Center for Computer Science
University of Kentucky, Lexington, Kentucky 40506

Received April 16, 2001

Revised Manuscript Received August 21, 2001

Single-walled carbon nanotubes (SWNTs) are expected to have a rich chemistry,¹ and the development of this subject will make available a unique set of materials.^{1–5} We have shown that chemical processing of short (100–300 nm in length⁶) SWNTs allows the preparation of stable organic solutions of these materials.^{6,7} Related routes to soluble SWNTs have been reported,⁸ together with approaches involving side-wall functionalization.⁹ To systematize the chemistry of SWNTs, it is necessary to develop analytical tools for the detection and identification of the different species of SWNTs. Raman spectroscopy and near-infrared (NIR) spectroscopy have already been very useful in this regard.

The Raman spectroscopy of SWNTs usually consists of the tangential- and radial-mode vibrations,¹⁰ of frequency ω_t and ω_r , respectively (Figure 1). The radial-mode frequency can be related to the diameter (d , nm) of the SWNT via the relationship $\omega_r = 223.75 \text{ (nm}\cdot\text{cm}^{-1})/d$.¹¹ The electronic spectra of SWNTs show transitions in the visible and NIR regions of the electromagnetic spectrum, and they may be observed in solutions or films of the SWNTs.¹² These electronic transitions occur between singularities in the density of states of the band structure of the SWNTs.^{3,13,14}

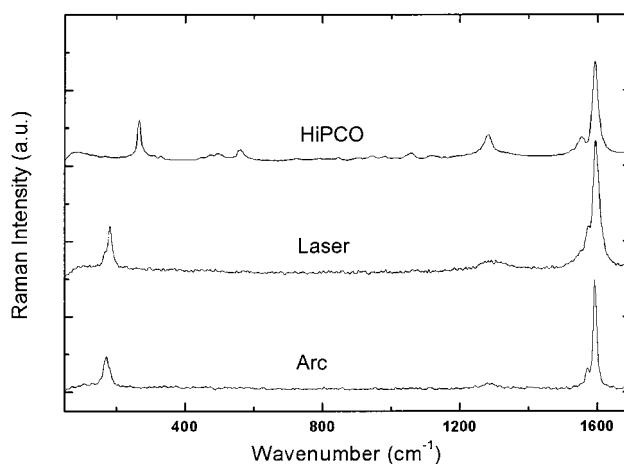


Figure 1. Raman spectra (Bruker RFS100/S spectrometer) of films of purified HiPCO, purified Laser, and soluble Arc produced SWNTs excited at 1064 nm (1.17 eV).

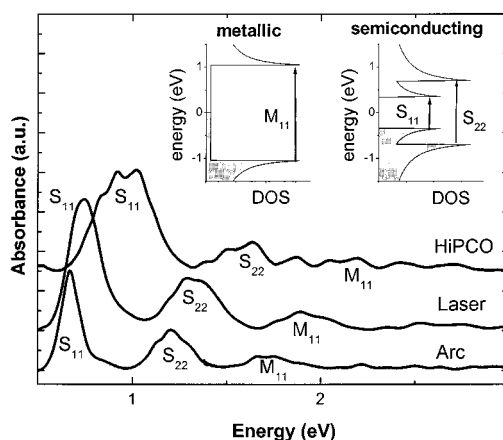


Figure 2. Absorption spectra (Varian Cary 500 spectrometer) of films of purified HiPCO, purified Laser, and soluble Arc produced SWNTs after baseline correction.

We refer to these as band gap transitions in both the semiconducting (S) and metallic (M) SWNTs (Figure 2). Within simple tight-binding (STB) theory (equivalent to HMO theory), in which the electronic band structure is assumed to arise from a pure p-orbital at each conjugated carbon atom (σ, π separability),¹⁵ the low-energy band gap transitions take a simple analytical form:³ $S_{11} = 2a\beta/d$, $S_{22} = 4a\beta/d$, $M_{11} = 6a\beta/d$, where a is the carbon-carbon bond length (nm), β (sometimes symbolized as γ) is the transfer or resonance integral between the p π -orbitals ($\beta = 2.9$ eV), and d is the diameter (nm) of the particular semiconducting or metallic SWNT.

Thus, according to theory, both the Raman radial-mode frequency and the electronic band transitions depend inversely on the diameter of the SWNTs. In the present communication we obtain the diameters of SWNT preparations from the Raman radial-mode frequencies and use this information to calibrate the TB p-orbital calculations against our measurements of the electronic band structures of these materials. We find significant deviations in the case of small-diameter SWNTs that are best explained by rehybridization effects.^{13,16}

The samples used in the study were commercial preparations obtained from Carbon Solutions, Inc. (electric arc),¹⁷ Tubes @Rice

(15) Haddon, R. C. *Acc. Chem. Res.* **1988**, *21*, 243–249.

(16) Blase, X.; Benedict, L. X.; Shirley, E. L.; Louie, S. G. *Phys. Rev. Lett.* **1994**, *72*, 1878–1881.

[†] University of California.

[‡] Versilant Nanotechnologies LLC.

[§] University of Kentucky.

(1) Chen, Y.; Haddon, R. C.; Fang, S.; Rao, A. M.; Eklund, P. C.; Lee, W. H.; Dickey, E. C.; Grulke, E. A.; Pendergrass, J. C.; Chavan, A.; Haley, B. E.; Smalley, R. E. *J. Mater. Res.* **1998**, *13*, 2423–2431.

(2) Thess, A.; Lee, R.; Nikolaev, P.; Dai, H.; Petit, P.; Robert, J.; Xu, C.; Lee, Y. H.; Kim, S. G.; Rinzler, A. G.; Colbert, D. T.; Scuseria, G. E.; Tomanek, D.; Fischer, J. E.; Smalley, R. E. *Science* **1996**, *273*, 483–487.

(3) Dresselhaus, M. S.; Dresselhaus, G.; Eklund, P. C. *Science of Fullerenes and Carbon Nanotubes*; Academic: San Diego, 1996.

(4) Wong, E. W.; Sheehan, P. E.; Lieber, C. M. *Science* **1997**, *277*, 1971–1975.

(5) Frank, S.; Poncharal, P.; Wang, Z. L.; de Heer, W. A. *Science* **1998**, *280*, 1744–1746.

(6) Chen, J.; Hamon, M. A.; Hu, H.; Chen, Y.; Rao, A. M.; Eklund, P. C.; Haddon, R. C. *Science* **1998**, *282*, 95–98.

(7) Hamon, M. A.; Chen, J.; Hu, H.; Chen, Y.; Rao, A. M.; Eklund, P. C.; Haddon, R. C. *Adv. Mater.* **1999**, *11*, 834–840.

(8) Riggs, J. E.; Guo, Z.; Carroll, D. L.; Sun, Y.-P. *J. Am. Chem. Soc.* **2000**, *122*, 5879–5880.

(9) Mickelson, E. T.; Chiang, I. W.; Zimmerman, J. L.; Boul, P. J.; Lozano, J.; Liu, J.; Smalley, R. E.; Hauge, R. H.; Margrave, J. L. *J. Phys. Chem. B* **1999**, *103*, 4318–4322.

(10) Rao, A. M.; Richter, E.; Bandow, S.; Chase, B.; Eklund, P. C.; Williams, K. A.; Fang, S.; Subbaswamy, K. R.; Menon, M.; Thess, A.; Smalley, R. E.; Dresselhaus, G.; Dresselhaus, M. *Science* **1997**, *275*, 187–191.

(11) Bandow, S.; Asaka, S.; Saito, Y.; Rao, A. M.; Grigorian, L.; Richter, E.; Eklund, P. C. *Phys. Rev. Lett.* **1998**, *80*, 3779–3782.

(12) Chen, J.; Rao, A. M.; Lyuksyutov, S.; Itkis, M. E.; Hamon, M. A.; Hu, H.; Cohn, R. W.; Eklund, P. W.; Colbert, D. T.; Smalley, R. E.; Haddon, R. C. *J. Phys. Chem. B* **2001**, *105*, 2525–2528.

(13) Odom, T. W.; Hiang, J.-L.; Kim, P.; Lieber, C. M. *J. Phys. Chem. B* **2000**, *104*, 2794–2809.

(14) Katura, H.; Kumazawa, Y.; Maniwa, Y.; Umezui, I.; Suzuki, S.; Ohtsuka, Y.; Achiba, Y. *Synth. Met.* **1999**, *103*, 2555–2558.

Table 1. Spectroscopic Results

Raman frequencies and calculated diameters	vis-NIR electronic transitions		arc value scaled by diameter	% diff. to scaled arc value
	type	(eV)		
	arc			
$\omega_i = 1594.1 \text{ cm}^{-1}$	S ₁₁	0.67		
$\omega_t = 169.8 \text{ cm}^{-1}$	S ₂₂	1.11		
$d = 1.318 \text{ nm}$	S ₂₂	1.21		
	S ₂₂	1.31		
	M ₁₁	1.66		
	M ₁₁	1.74		
	M ₁₁	1.90		
	laser			
$\omega_i = 1593.5 \text{ cm}^{-1}$	S ₁₁	0.76	0.72	-6
$\omega_t = 181.5 \text{ cm}^{-1}$	S ₂₂	1.16	1.19	2
$d = 1.233 \text{ nm}$	S ₂₂	1.30	1.29	-1
	S ₂₂	1.36	1.40	3
	M ₁₁	1.74	1.77	2
	M ₁₁	1.89	1.86	-2
	M ₁₁	2.02	2.03	1
	HiPCO			
$\omega_i = 1594.7 \text{ cm}^{-1}$	S ₁₁	0.82		
$\omega_t = 266.7 \text{ cm}^{-1}$	S ₁₁	0.91	1.05	14
$d = 0.839 \text{ nm}$	S ₁₁	1.01		
	S ₂₂	1.38	1.74	21
	S ₂₂	1.50	1.90	21
	S ₂₂	1.62	2.06	21
	M ₁₁	1.86	2.61	29
	M ₁₁	2.02	2.73	26
	M ₁₁	2.17	2.98	27

(laser oven),² and Carbon Nanotechnologies (HiPCO; 10 atm material).¹⁸ Solutions (suspensions) of each sample were sprayed, via nitrogen gas, onto glass substrates heated between 180 and 200 °C until dark, homogeneous films were produced.

The frequencies^{10,12,19} and calculated diameters of the SWNTs are summarized in the Table 1. Laser excitation at 1064 nm provides Raman spectroscopic information on the semiconducting and not the metallic SWNTs, but the diameter distributions are expected to be similar within any given sample. For comparison purposes, we include the literature diameters (d) for the SWNT samples: 1.34 (0.13) nm (arc), 1.21 (0.07) nm (laser), and 0.81 (0.08) nm (HiPCO), as obtained by transmission electron microscopy and X-ray diffraction,^{18,20,21} where the numbers correspond to the mean value and the standard deviation (σ) of the diameter distributions.

Our analysis focuses on the three most prominent nanotubes in each SWNT sample; on the basis of the energy distribution of these peaks in the electronic spectra and the statistical analysis given above, we conclude that these three SWNTs fall well within 1 standard deviation (σ) of the sample populations of all three materials. On the basis of a Gaussian distribution of SWNT diameters we conclude that our analysis includes ~70% of the samples.

(17) Journet, C.; Maser, W. K.; Bernier, P.; Loiseau, A.; Lamy de la Chapelle, M.; Lefrant, S.; Deniard, P.; Lee, R.; Fischer, J. E. *Nature* **1997**, *388*, 756–758.

(18) Nikolaev, P.; Bronikowski, M. J.; Bradley, R. K.; Rohmund, F.; Colbert, D. T.; Smith, K. A.; Smalley, R. E. *Chem. Phys. Lett.* **1999**, *313*, 91–97.

(19) Rao, A. M.; Chen, J.; Richter, E.; Eklund, P. C.; Haddon, R. C.; Venkateswaran, U. D.; Kwon, Y.-K.; Tomaneck, D. *Phys. Rev. Lett.* **2001**, *86*, 3895–3898.

(20) Rinzler, A. G.; Liu, J.; Dai, H.; Nilolaev, P.; Huffman, C. B.; Rodriguez-Macias, F. J.; Boul, P. J.; Lu, A. H.; Heymann, D.; Colbert, D. T.; Lee, R. S.; Fischer, J. E.; Rao, A. M.; Eklund, P. C.; Smalley, R. E. *Appl. Phys. A* **1998**, *67*, 29–37.

(21) Ichida, M.; Mizuno, S.; Tani, Y.; Saito, Y.; Nakamura, A. *J. Phys. Soc. Jpn.* **1999**, *68*, 3131–3133.

The TB calculations by Charlier for the (12,8) semiconducting and (10,10) metallic SWNTs ($S_{11} = 0.7 \text{ eV}$, $S_{22} = 1.2 \text{ eV}$ and $M_{11} = 1.7 \text{ eV}$)²² give band gap transitions in excellent agreement with our experimental results for the arc-produced material. Nevertheless, these experimental and theoretical results make clear that the STB calculations (above) are incapable of quantitatively accounting for the electronic transitions in SWNTs, although the qualitative trend is correctly reproduced. For example, application of the STB formulas (above) would suggest that the ratios of the excitation energies should be: $S_{11}:S_{22}:M_{11} = 1:2:3$, whereas both experiment and detailed calculation give: $S_{11}:S_{22}:M_{11} = 1:1.7:2.4$. Nevertheless, even sophisticated theories support the idea that the electronic transition energies depend inversely on nanotube diameter if σ, π -separability is maintained.³

Thus, we took the electronic band transitions of the arc-produced SWNTs as reference and using the diameters obtained from the Raman spectra, scaled these values to the diameters obtained for the laser- and HiPCO-produced material, and included them in our table of results (last two columns). Clearly, there is very good agreement (within 6%) between the measured electronic spectra of the laser-produced material and the values calculated from the arc-produced material by scaling with the diameters derived from the Raman spectra. However, in the case of the HiPCO-produced material the scaled values are uniformly greater in energy than the experimental values by about 20%.

As a result of rehybridization (mixing of s -character into the π^* -orbitals), LDA calculations predict that the states in the conduction band will be lower in energy than those estimated by p -orbital TB calculations;^{13,16} exactly the same mechanism contributes to the high electron affinity of the fullerenes.²³ Clearly our results bear out this prediction. Thus, we can expect an increased reactivity²⁴ due to strain in the HiPCO-produced SWNTs together with an enhanced electron affinity over the larger diameter SWNTs that are produced in the arc and the laser methods. For comparison purposes we note that the pyramidalization angles (θ_p , deg) and the π -orbital misalignment angles (ϕ , deg) in C_{60} are $\theta_p = 11.64$ and $\phi = 0$,^{25–27} whereas representative SWNTs give values: (20, 0), (diameter), $d = 15.61 \text{ \AA}$, $\theta_p = 2.59$, $\phi = 0$, 9.1; (18, 0), $d = 14.05$, $\theta_p = 2.88$, $\phi = 0$, 10.1; (16, 0), $d = 12.49$, $\theta_p = 3.24$, $\phi = 0$, 11.4; (14, 0), $d = 10.93$, $\theta_p = 3.69$, $\phi = 0$, 13.1; (12, 0), $d = 9.37$, $\theta_p = 4.30$, $\phi = 0$, 15.3; (10, 0), $d = 7.81$, $\theta_p = 5.15$, $\phi = 0$, 18.5; (10, 10), $d = 13.52$, $\theta_p = 3.00$, $\phi = 0$, 10.4; (9, 9), $d = 12.17$, $\theta_p = 3.33$, $\phi = 0$, 11.6; (8, 8), $d = 10.82$, $\theta_p = 3.74$, $\phi = 0$, 13.1; (7, 7), $d = 9.47$, $\theta_p = 4.27$, $\phi = 0$, 15.0; (6, 6), $d = 8.11$, $\theta_p = 4.99$, $\phi = 0$, 17.6; (5, 5), $d = 6.76$, $\theta_p = 5.97$, $\phi = 0$, 21.3. It is interesting to note that the strain in carbon nanotubes arises from a combination of π -orbital misalignment²⁸ and pyramidalization, whereas it is almost exclusively due to pyramidalization in the fullerenes.^{1,27}

Acknowledgment. This work was supported by the MRSEC Program of the National Science Foundation under Award Number DMR-9809686, and by the Office of Naval Research under Award Number N00014-99-1-0770.

JA0109702

(22) Ajayan, P. M. *Chem. Rev.* **1999**, *99*, 1787–1799.

(23) Haddon, R. C. *Acc. Chem. Res.* **1992**, *25*, 127.

(24) Bahr, J. L.; Yang, J.; Kosynkin, D. V.; Bronikowski, M. J.; Smalley, R. E.; Tour, J. M. *J. Am. Chem. Soc.* **2001**, *123*, 6536–6542.

(25) Haddon, R. C.; Brus, L. E.; Raghavachari, K. *Chem. Phys. Lett.* **1986**, *125*, 459–464.

(26) Haddon, R. C. *J. Am. Chem. Soc.* **1987**, *109*, 1676–1685.

(27) Haddon, R. C. *Science* **1993**, *261*, 1545–1550.

(28) Kleiner, A.; Eggert, S. *Phys. Rev. B* **2001**, *63*, 073408.